Journal of Solid State Chemistry **166,** 279–284 (2002)
doi:10.1006/jssc.2002.9585

A Suberato-Pillared Mn(II) Coordination Polymer: Hydrothermal Synthesis, Crystal Structure, and Magnetic Properties of $Mn_2(H_2O)[O_2C(CH_2)_6CO_2]_2$

Yue-Qing Zheng[1] and Zu-Ping Kong

Municipal Key Laboratory of Inorganic Materials Chemistry, Institute for Solid State Chemistry, Ningbo University, Ningbo 315211, People's Republic of China

Received November 12, 2001; in revised form March 4, 2002; accepted March 15, 2002

A suberato-pillared Mn(II) coordination polymer $Mn_2(H_2O)(C_8H_{12}O_4)_2$ was hydrothermally synthesized at 170°C for 3 days and characterized by single-crystal X-ray diffraction. Crystal data: monoclinic, $C2/c$, $Z = 4$, $a = 26.544(5)$, $b = 7.617(2)$, $c = 9.187(2)$ Å, $\beta = 105.38(2)°$, $V = 1791.0(7)$ Å^3, $R_1 = 0.064$ and w$R_2 = 0.162$. The compound shows a layered structure consisting of inorganic Mn oxygen polyhedral layers and organic regions. The inorganic Mn oxygen layers are generated from Mn_2O_{10} bioctahedral units, which share corners with neighbors to form zigzag chains along the [001] direction and are, along the [010] direction, further connected by carboxylate groups of the suberato ligands and hydrogen bonds. The magnetic studies indicated that the compound becomes antiferromagnetic at low temperatures with $T_{Néel} = 12$ K and follows Curie–Weiss law $\chi_m(T + 22.429) = 4.48\,cm^3\,mol^{-1}\,K$ between 25 and 300 K. Upon heating in Ar stream, $Mn_2(H_2O)(C_8H_{12}O_4)_2$ decomposes in three steps.

Key Words: **manganese(II); coordination polymer; hydrothermal synthesis; crystal structure; properties.**

INTRODUCTION

Rational design and syntheses of coordination polymers with specific topologies are currently of growing interest due to their promising properties for potential technological and industrial applications (1). An important synthetic strategy for such compounds extensively utilizes the bifunctional rigid bridging ligands (2). In recent years, our research has been intensively focused on exploitation of polydentate saturated α,ω-dicarboxylate anions as flexible spacers to construct supramolecular architectures. Under ambient conditions, self-assemblies of transition metal ions with α,ω-dicarboxylate anions yielded 0D discrete complex molecule and a variety of coordination polymers ranging from 1D chains through 2D layers to 3D networks. To our knowledge, the $Ag_4(C_5H_6O_4)_2$ complex gives a unique example of 0D discrete complex molecule, where the bent glutarate anions act as bis-bidentate ligands (3). On the other hand, bis-monodentate dicarboxylato ligands could bridge metal atoms into catena polymeric chains (4). Polymeric chains could be also generated from metal atoms bridged by bidentate carboxylato groups of dicarboxylate anions (5). When metal atoms are bridged by double bis-monodentate dicarboxylato ligands, 1D polymeric anionic chains with rings could be formed (6). Such anionic chains, in some cases, could be further interlinked by metal cations into 2D neutral open networks (7). Furthermore, the Cu_2 dimeric units in $Cu(C_4H_4O_4)\cdot 2H_2O$ are bridged by double bis-bidentate succinato ligands, resulting in 1D chains (8). Self-assembly of Mn(II) ions with sebacate anions resulted in the formation of 1D ribbon-like chains (9). In comparison with 1D catena polymers, metal dicarboxylates with 2D layers are relatively rare. Two Cd succinates are found to consist of 2D open layers resulting from Cd atoms interlinked by polydentate succinato ligands (10). Interestingly, suberate anions coordinate Co atoms to form trilayers with two Co oxygen polyhedral layers pillared by suberato ligands (11). In addition, self-assembly of Zn(II) ions with dicarboxylate anions afforded coordination polymers with 3D diamondoid networks resulting from Zn atoms interlinked by bis-bidentate ligands (12). In $Ag_2(C_4H_4O_4)$, however, 3D diamondoid networks from the Ag_4 rhombus clusters bridged by bis-bidentate succinato ligands interpenetrate with one another (13). Furthermore, synergetic coordination of hydroxo and succinato ligands assembles Co atoms to yield 3D open frameworks and guest molecules fill void spaces (14). Our previous studies indicated that the seemingly simple synthetic strategy based on self-assembly

[1]To whom correspondence should be addressed. Fax: Int. +574/87600747. E-mail: zhengcm@nbu.edu.cn.

0022-4596/02 $35.00

of transition metal ions with dicarboxylate ions could provide an interesting route to advanced materials, for example, the Zn succinate exhibits strong secondary harmonic generation (SHG) effects (12a,b). As an ongoing part of our research project on coordination chemistry of saturated α,ω-dicarboxylates, we report herein a suberato-pillared Mn(II) coordination polymer $Mn_2(H_2O)(C_8H_{12}O_4)_2$, which was hydrothermally synthesized at 170°C for 3 days and behaves antiferromagnetically at low temperature.

EXPERIMENTAL

All chemicals of p.a. grade were commercially available and used without further purification. The C and H microanalyses were performed with a Heraeus Rapid-CHNO elemental analyzer. The FT–IR spectra were recorded from KBr pellets in the range 4000–400 cm^{-1} on a Protege 460 spectrometer. The magnetic susceptibility was measured on a powdered sample (63.04 mg) using a SQUID magnetometer (Quantum Design Model MPMS-7) in temperature range $5 \leq T(K) \leq 300$ with an applied field of 10,000 G. The susceptibility was corrected for diamagnetic contributions by using Pascal constant $\chi_{dia.} = -70 \times 10^{-6}$ cm^3 mol^{-1} (15). The thermogravimetric analyses (TG) was carried out between 25 and 800°C on a pre-weighed sample (19.90 mg) in flowing Ar using a WCT-2A thermogravimeter (Beijing Optical Instrument Co.) with a heating rate of 5°C min^{-1}.

SYNTHESES

The synthetic procedure was optimized as follows. Addition of 2.0 mL (1 M) Na_2CO_3 to an aqueous solution of $MnSO_4 \cdot H_2O$ (0.17 g, 1.0 mmoL) in 6.0 ml H_2O produced white precipitate, which was then separated and washed by doubly distilled water until no detectable SO_4^{2-} anions. Under continuous stirring, the fine precipitate was added to suberic acid (0.53 g, 3.0 mmoL) in 15 ml H_2O. The mixture was further stirred for ca. 30 min. The formed suspension (pH = 4.73) was then moved to a 23 mL Teflon-lined stainless-steel vessels and heated at 170°C for 3 days. After cooling, the solid was filtered out and excess suberic acid was leached out by ethanol, affording faintly reddish plate-like crystals of the title compound. The yield reached over 75% based on the initial $MnSO_4 \cdot H_2O$ input. Anal. Calc. for $C_{16}H_{26}Mn_2O_9$ (%): C, 40.69; H, 5.55. Found: C, 40.73; H, 5.61. IR (cm^{-1}): 3035 vs, 3974 s, 2930 vs, 2854 vs, 2494 vw, 2340 vw, 1562 vs, 1404 vs, 1351 vs, 1334 vs, 1288 vs, 1245 vs, 1217 m, 1199 m, 1134 w, 1081 m, 1049 s, 1022 vw, 1000 vw, 973 vw, 949 vw, 936 vw, 871 w, 797 s, 775 m, 743 m, 728 s, 726 vs, 655 vs, 574 w, 551 w, 484 vw, 435 m, 409 w.

X-RAY CRYSTALLOGRAPHY

Suitable single crystal was selected under a polarizing microscope and fixed with epoxy cement on a fine glass fiber which was then mounted on a Bruker P4 diffractometer with graphite-monochromated Mo$K\alpha$ radiation ($\lambda = 0.71073$ Å) for cell determination and subsequent data collection. The lattice parameters were refined from the 2ϑ values (10–25°) of 25 carefully centered reflections. The reflection intensities with $2\vartheta_{max} = 55°$ were collected at 293 K using the $\vartheta - 2\vartheta$ scan technique. On the basis of the monitored reflections, the employed single crystal exhibits no detectable decay during the data collection. The data were corrected for Lp and absorption effects. SHELXS-97 and SHELXL-97 programs (16, 17) were used for structure solution and refinement. The structure was solved by using direct methods. Subsequent difference Fourier syntheses enabled all non-hydrogen atoms to be located. After several cycles of refinement, all hydrogen atoms were located from the successive difference Fourier syntheses. Finally, all non-hydrogen atoms were refined with anisotropic displacement parameters by full-matrix least-squares technique and hydrogen atoms with isotropic displacement parameters. Detailed information about the crystal data and structure determination is summarized in Table 1. Atomic coordinates, equivalent isotropic displacement parameters are listed in Table 2. Selected interatomic distances and bond angles are given in Table 3. Crystallographic data (excluding structure factors) for the structures in this paper have been deposited with Cambridge Crystallographic Data Centre as supplementary publication nos. CCDC 180093 ($C_{16}H_{26}Mn_2O_9$). Copies of the data can be obtained, free of charge, on application to CCDC, 12 Union Road, Cambridge CB2 1EZ, UK (fax: +44 1223 336033 or e-mail: deposit@ccdc.cam.ac.uk).

RESULTS AND DISCUSSION

Syntheses

Repeated experiments envidenced that the title compound could not be obtained under ambient conditions. The plate-like crystals of the title compound resulting from hydrothermal reactions of the fresh $MnCO_3 \cdot xH_2O$ precipitate and suberic acid in the molar ratio from 1 : 1 to 1 : 2.5 were severely contaminated by dark brown Mn_3O_4. The formation of Mn_3O_4 could be completely suppressed by increasing the molar ratio of $MnCO_3 \cdot xH_2O$ and suberic acid to 1 : 3. The title compound was found to be stable in water and some polar organic solvents such as ethanol, methanol and acetonitrile so that leaching excess suberic acid out with ethanol could readily purify the product.

TABLE 1
Summary of Crystal Data, Data Collection, Structure Solution, and Refinement Details for $Mn_2(H_2O)(C_8H_{12}O_4)_2$

Empirical formula	$C_{16}H_{26}Mn_2O_9$
Formula weight	472.25
Description	Faintly redish thin plate
Crystal size (mm)	$0.556 \times 0.333 \times 0.067$
Temperature	293(2)
Crystal system	Monoclinic
Space group	$C2/c$
Unit-cell dimensions	
a (Å)	26.544(5)
b (Å)	7.617(2)
c (Å)	9.187(2)
β (°)	105.38(2)
Volume (Å^3)	1791.0(7)
Z	4
D_{calc} (g cm^{-3})	1.751
$F(0\,0\,0)$	976
Absorption coefficient (mm^{-1})	1.459
Absorption correction	Empirical
Maximum and minimum transmission	0.513, 0.993
θ Range (°)	0.45–27.50
Refinement method	Full-matrix least-squares on F^2
Reflections collected	2383
Independent reflections (R_{int})	1981 (0.0257)
Data/restraints/parameters	1797/0/174
Goodness of fit on F^2	1.075
R_1, w$R_2[I \geq 2\sigma(I)]^a$	0.0639, 0.1622
R_1, wR_2 (all data)^a	0.0667, 0.1666
A, B values in weighting scheme^b	0.1415, 0.0000
Largest difference peak and hole (e Å^{-3})	3.135, −1.273

^{a}w$R_2 = [\sum w(F_o^2 - F_c^2)^2 / \sum w(F_o^2)^2]^{1/2}$.
^{b}w $= [\sigma^2(F_o^2) + (AP)^2 + BP]^{-1}$ with $P = (F_o^2 + 2F_c^2)/3$.

Crystal Structure

The basic building blocks in the title compound are the edge-shared Mn_2O_{10} bioctahedra. Just as demonstrated in Fig. 1, the Mn atoms are each coordinated by one water oxygen atom and five carboxylate oxygen atoms from different suberato ligands to complete MnO_6 octahedral geometry. The Mn–O bond distances vary in the range 2.129–2.385 Å with the largest one to the water molecule and the transoid and cisoid O–Mn–O bond angles exhibit significant deviation from 180 and 90°, respectively (Table 3), which suggests the MnO_6 octahedra to be strongly distorted. The present Mn–to–O distances are comparable with some known manganesed dicarboxylates, e.g. 2.179–2.243 Å in $Mn(C_4H_4O_4)\cdot 4H_2O$ (4a), 2.156–2.255 Å in $Mn(H_2O)_4(C_4H_4O_4)$ (4e), 2.136–2.196 Å in $Mn(H_2O)_4(C_5H_6O_4)$ (5), and 2.118–2.267 Å in $Mn(H_2O)_3(C_{10}H_{16}O_4)$ (9).

Two adjacent MnO_6 octahedra are condensed via two carboxylate O atoms to form Mn_2O_{10} bioctahedra centered at the crystallographic 4*b* positions. The Mn···Mn separation within the bioctahedron is of 3.400(1) Å. As demonstrated in Fig. 2, neighboring bioctahedra share the water molecules and at the same time are doubly bridged by carboxylate groups, leading to a zigzag chain along the [0 0 1] direction. The resulting chains, along the [0 1 0] direction, are further doubly bridged by carboxylate groups to form 2D Mn–O layers parallel to (1 0 0). The connection of the zigzag chains are reinforced by hydrogen bonds existing between water molecule and carboxylate O atoms of neighboring chains ($d(O5\cdots O3^{IX}) = 2.739$ Å, $\angle(O5\text{–}H\cdots O3^{IX}) = 157°$, ^{IX}: $\frac{1}{2}-x$, $\frac{1}{2}-y$, $1-z$). Within the chain, the closest inter-bioctahedral Mn···Mn distance of 3.648(1) Å is substantially smaller than the nearest inter-chain distance of 4.727(1) Å. The alkyl chains connect the inorganic layers. The inorganic layer is shifted by $\frac{1}{2}\vec{b}$ with respect to the next inorganic layer. The alkyl chains between the inorganic layers orientate neraly parallelly and

TABLE 2
Atomic Parameters and Equivalent Isotropic Thermal Parameters (Å^2) for Non-hydrogen Atoms in $Mn_2(H_2O)(C_8H_{12}O_4)_2$

Atom	Wyckoff site	x	y	z	Ueq
Mn	8*f*	0.01774(1)	0.20353(5)	0.45589(4)	0.0124(2)
C(1)	8*f*	0.07659(9)	−0.0192(3)	0.7444(3)	0.0113(5)
C(2)	8*f*	0.1277(1)	0.0458(4)	0.7219(3)	0.0179(6)
C(3)	8*f*	0.1761(1)	0.0091(4)	0.8502(3)	0.0187(6)
C(4)	8*f*	0.2263(1)	0.0460(5)	0.8052(3)	0.0210(6)
C(5)	8*f*	0.2755(1)	0.0161(4)	0.9334(3)	0.0202(6)
C(6)	8*f*	0.3261(1)	0.0455(5)	0.8877(3)	0.0214(6)
C(7)	8*f*	0.3747(1)	0.0205(4)	1.0195(3)	0.0177(6)
C(8)	8*f*	0.4242(1)	0.0490(4)	0.9691(3)	0.0131(5)
O(1)	8*f*	0.03504(7)	0.0191(2)	0.6413(2)	0.0148(4)
O(2)	8*f*	0.07654(7)	−0.1126(3)	0.8554(2)	0.0179(4)
O(3)	8*f*	0.44165(8)	−0.0805(3)	0.9086(2)	0.0173(4)
O(4)	8*f*	0.44437(9)	0.1984(3)	0.9840(3)	0.0211(5)
O(5)	4*e*	0	0.4052(4)	$\frac{1}{4}$	0.0169(6)

Note. U_{eq} is defined as one-third of the trace of the orthogonalized U_{ij} tensor.

TABLE 3
Selected Interatomic Distances (Å) and Bond Angles (°) for $Mn_2(H_2O)(C_8H_{12}O_4)_2$

Mn–O(1)	2.161(2)	C(3)–C(4)	1.525(4)
Mn–O(1)$^{\#1}$	2.230(2)	C(4)–C(5)	1.524(4)
Mn–O(2)$^{\#6}$	2.129(2)	C(5)–C(6)	1.528(4)
Mn–O(3)$^{\#7}$	2.169(2)	C(6)–C(7)	1.528(4)
Mn–O(4)$^{\#8}$	2.164(2)	C(7)–C(8)	1.520(3)
Mn–O(5)	2.385(2)	C(8)–O(3)	1.278(4)
C(1)–O(1)	1.282(3)	C(8)–O(4)	1.250(3)
C(1)–O(2)	1.244(3)	Mn···Mn$^{\#1}$	3.400(1)
C(1)–C(2)	1.509(3)	Mn···Mn$^{\#2}$	3.648(1)
C(2)–C(3)	1.521(4)	Mn···Mn$^{\#9}$	4.727(1)
O(1)–Mn–O(1)$^{\#1}$	78.52(8)	O(2)$^{\#6}$–Mn–O(4)$^{\#8}$	161.89(9)
O(1)–Mn–O(2)$^{\#6}$	95.93(8)	O(2)$^{\#6}$–Mn–O(5)	83.04(6)
O(1)–Mn–O(3)$^{\#7}$	94.09(7)	O(3)$^{\#7}$–Mn–O(4)$^{\#8}$	89.75(8)
O(1)–Mn–O(4)$^{\#8}$	98.06(8)	O(3)$^{\#7}$–Mn–O(5)	85.99(7)
O(1)–Mn–O(5)	178.97(6)	O(4)$^{\#8}$–Mn–O(5)	82.97(7)
O(1)$^{\#1}$–Mn–O(2)$^{\#6}$	91.95(7)	Mn–O(1)–Mn$^{\#1}$	101.48(8)
O(1)$^{\#1}$–Mn–O(3)$^{\#7}$	166.00(8)	Mn–O(5)–Mn$^{\#2}$	99.8(1)
O(1)$^{\#1}$–Mn–O(4)$^{\#8}$	79.67(7)	O(1)–C(1)–O(2)	123.2(2)
O(1)$^{\#1}$–Mn–O(5)	101.61(7)	O(3)–C(8)–O(4)	123.7(3)
O(2)$^{\#6}$–Mn–O(3)$^{\#7}$	100.70(8)		

Torsion angles (°)

C(1)–C(2)–C(3)–C(4)	168.6(3)
C(2)–C(3)–C(4)–C(5)	178.1(3)
C(3)–C(4)–C(5)–C(6)	177.6(3)
C(4)–C(5)–C(6)–C(7)	178.2(3)
C(5)–C(6)–C(7)–C(8)	179.4(3)

Symmetry codes: #1 $-x, -y, -z+1$; #2 $-x, y, -z+\frac{1}{2}$; #3 $-x+\frac{1}{2}, y-\frac{1}{2}, -z+\frac{3}{2}$; #4 $x, -y, z+\frac{1}{2}$; #5 $x+\frac{1}{2}, -y+\frac{1}{2}, z+\frac{1}{2}$; #6 $x, -y, z-\frac{1}{2}$; #7 $-x+\frac{1}{2}, y+\frac{1}{2}, -z+\frac{3}{2}$; #8 $x-\frac{1}{2}, -y+\frac{1}{2}, z-\frac{1}{2}$; #9 $-x, -y+1, -z+1$

are arranged according to a pseudo close-packing pattern. The average distance between alkyl chains varies from 4.28 to 4.82 Å. Along the [100] direction, the inorganic layer and organic regions are alternated and stacked in a sequence of ···inorganic layer (A)···organic region (B)···inorganic layer (C)···organic region (D)··· (Fig. 3). Actually, the present coordination polymer could be viewed as the inorganic layers pillared by suberato ligands to form 3D framework with two kinds of tunnels extending infinitely in the [001] and [010] directions, respectively, and filled by alkyl hydrogen atoms (Fig. 3).

Each suberate anion coordinates to five Mn atoms, one carboxylate O atoms bridging two Mn atoms and the remaining three each bonded to one Mn atom. The backbone carbon atoms are nearly in a common plane, from which the terminal carboxylate groups are deviated to different extents (dihedral angles: 17.1(3) and 88.7(2)° for the carboxylate groups containing O(1) and O(3), respectively). Present coordinating mode of the suberato ligand differs from those observed in zinc suberate (12d) and cobalt suberate hydrate (11). In the former Zn salt, the suberate anions function as bis-bidentate ligands bridging metal atoms into a 3D diamondoid network similar to zinc succinate (12a, b) and zinc glutarate (12c). In the latter cobalt salt, both carboxylate groups of the dicarboxylato ligand behave differently, one chelating one Co atom and the other bidentately bridging two Co atoms. The formed Co oxygen polyhedral layers are pillared by suberato ligands. As a result, an inorganic–organic–inorganic trilayer is formed and the resulting trilayers are held together by hydrogen bonds (11).

Magnetic Properties

The temperature dependence of χ_m and χ_m^{-1} (χ_m and χ_m^{-1} being, respectively, the magnetic susceptibility and inverse magnetic susceptibility per Mn(II) ion) is shown in Fig. 4.

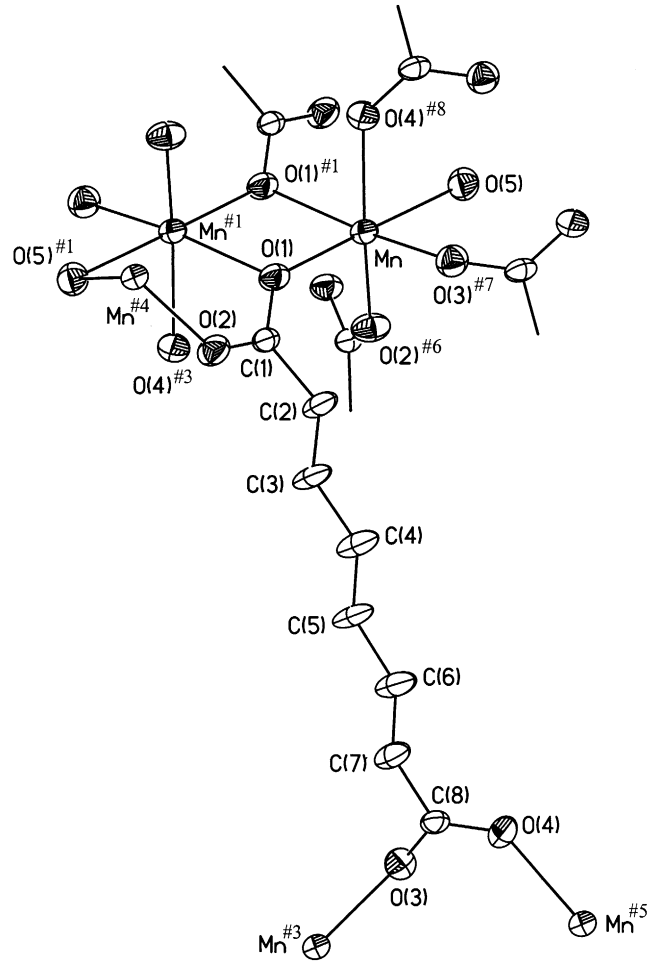

FIG. 1. Ortep view of bioctahedral Mn_2O_{10} dimers together with the coordinating suberato ligands and the atomic labelling. The displacement ellipsoids are drawn at 45% probability level (symmetry codes: see Table 3).

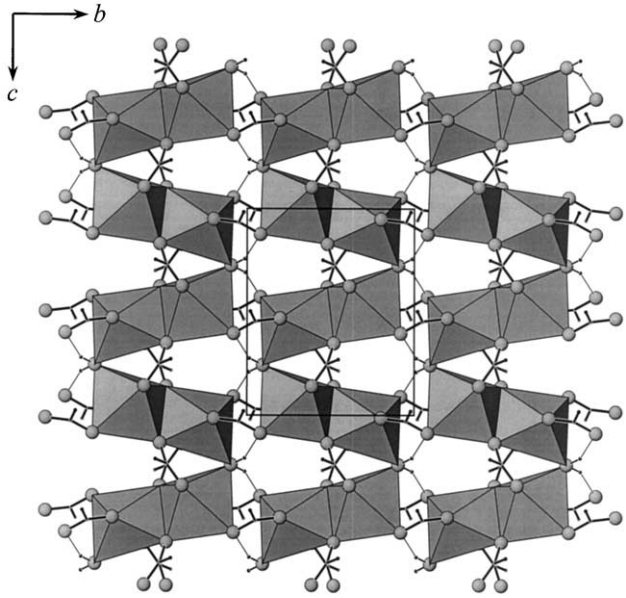

FIG. 2. Inorganic layer generated from the Mn_2O_{10} bioctahedra. The hydrogen bonds between water and carboxylate O atoms are indicated by thin lines.

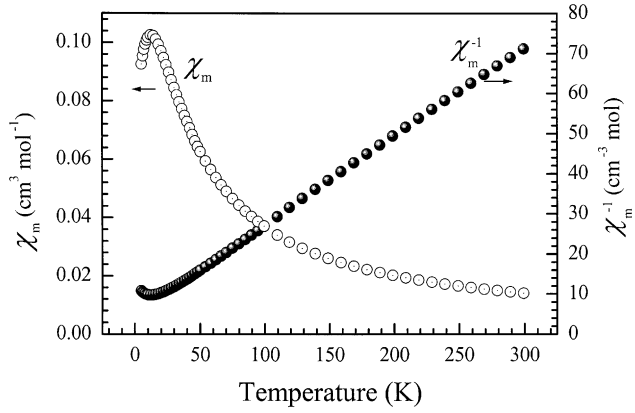

FIG. 4. Temperature dependences of the magnetic susceptibility $\chi_m/(cm^3\,mol^{-1})$ (per Mn^{II} ion) and the inverse magnetic susceptibility $\chi_m^{-1}/(cm^{-3}\,mol)$ (per Mn^{II} ion) for $Mn_2(H_2O)(C_8H_{12}O_4)_2$.

It is clear that the title compound becomes antiferromagnetic at low temperatures with a Néel temperature of 12 K. Between 25 and 300 K its magnetic behavior obeys Curie–Weiss law $\chi_m(T + 22.429) = 4.48\,cm^3\,mol^{-1}\,K$ with $\mu_{eff.} = 5.75$ B.M at room temperature. The observed magnetic moment is expected to be close to spin-only value (5.92 B.M.) for the octahedrally coordinated high-spin Mn(II) compound (18).

Thermal Analyses

The TG measurements carried out in flowing Ar between 25 and 800°C demonstrate that the title compound decomposes in three steps. Dehydration proceeds over 180–240°C with an observed weight loss of 3.92% in good agreement with the calculated value of 3.81% for one mole H_2O per formula. Upon further heating, the sample underwent a sharp weight loss at 285°C with an additional weight loss of 35.03% at 393°C corresponding well with the release of two moles of "C_6H_{12}" (calculated value: 35.65%). Up to 470°C, the weight loss reached 69.50% with MnO residue in an excellent accordance with the complete decomposition (calc. 69.96%). The last decom-

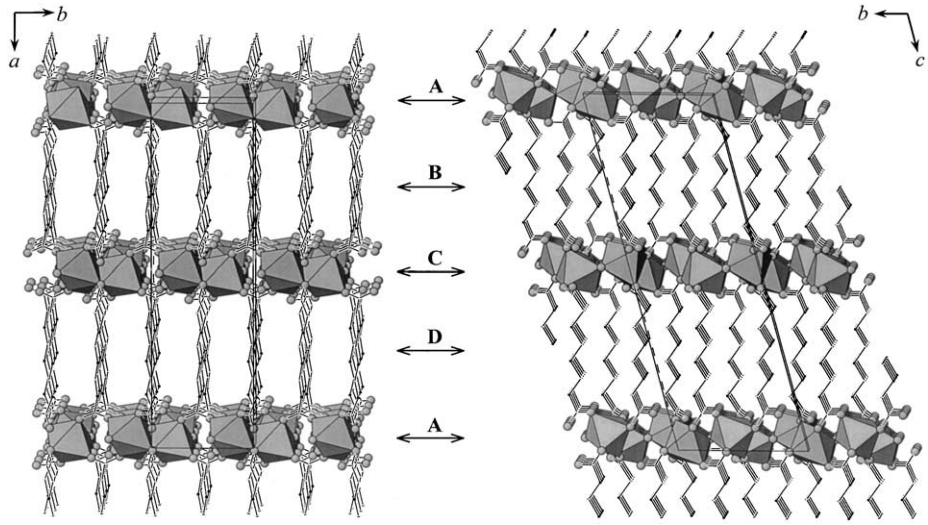

FIG. 3. Crystal structure of $Mn_2(H_2O)(C_8H_{12}O_4)_2$ projected along [0 0 1] and [0 1 0] directions, respectively, with two kinds of tunnels indicated.

position could be ascribed to that of Mn oxalate formed at the second step, which was verified by an additional thermogravimetric measurements on a freshly prepared $MnC_2O_4 \cdot 2H_2O$ sample.

ACKNOWLEDGMENTS

The project was supported by the Zhejiang Provincial Natural Science Foundation of P. R. China (RC99034) and Ningbo Municipal Natural Science Foundation (01J20130-1). The authors are indebted to Mr. Jian-Li Lin for X-ray diffraction data collection.

REFERENCES

1. B. Moulton and M. J. Zaworotko, *Chem. Rev.* **101,** 1629 (2001) and references therein.
2. (a) G. F. Swiegers and T. J. Malefeste, *Chem. Rev.* **100,** 3483 (2000); (b) C. Kaes, A. Katz, and M. W. Hosseini, *Chem. Rev.* **100,** 3553 (2000).
3. A. Michaelides, S. Skoulika, V. Kiritsis, and A. Aubry, *J. Chem. Soc., Chem. Commun.* 1415 (1995).
4. (a) M. P. Gupta, R. D. Sahu, R. Ram, and P. R. Maulik, *Z. Kristallogr.* **163,** 155 (1983); (b) E. Suresh, M. M. Bhadbhade, and K. Venkatasubramanian, *Polyhedron* **18,** 657 (1999); (c) Y.-Q. Zheng and J.-L. Lin, *Z. Kristallogr. NCS* **215,** 157 (2000); (d) Y.-Q. Zheng and J.-L. Lin, *Z. Kristallogr. NCS* **215,** 159 (2000); (e) M. Fleck, E. Tillmanns, and L. Bohaty, *Z. Kristallogr. NCS* **215,** 429 (2000); (f) Y.-Q. Zheng, A.-Y. Pan, and J.-L. Lin, *Z. Kristallogr. NCS* **216,** 263 (2001).
5. Y.-Q. Zheng, J.-L. Lin, J. Sun, and H.-L. Zhang, *Z. Kristallogr. NCS* **215,** 163 (2000).
6. (a) Y.-Q. Zheng and J.-L. Lin, *Z. Kristallogr. NCS* **215,** 165 (2000); (b) Y.-Q. Zheng, J.-L. Lin, and W.-J. Chen, *Z. Kristallogr. NCS* **216,** 269 (2001).
7. Y.-Q. Zheng, J.-L. Lin, and A.-Y. Pan, *Z. Anorg. Allg. Chem.* **626,** 1718 (2000).
8. B. H. O'Connor and E. N. Maslen, *Acta Crystallogr.* **20,** 824 (1966).
9. Y.-Q. Zheng, S.-Q. Zhou, and J.-L. Lin, *Z. Kristallogr. NCS* **216,** 265 (2001).
10. (a) E. A. H. Griffith, N. G. Charles, and E. L. Amma, *Acta Crystallogr. B* **38,** 262 (1966). (b) M. Fleck, E. Tillmanns, L. Bohaty, *Z. Kristallogr. NCS* **215,** 619 (2000).
11. Y.-Q. Zheng, J.-L. Lin, J. Sun, and A.-Y. Pan, *Z. Kristallogr. NCS* **215,** 161 (2000).
12. (a) Y.-Q. Zheng, K. Peters, and H. G. von Schnering, "12th International Conference on Solid Compounds of Transition Elements," Saint-Malo, France, Abstract-O10 (1997); (b) Y.-Q. Zheng, K. Peters, and H. G. von Schnering, *Chem. Res. Chinese Univ.* **17,** 19 (2001); (c) Y.-Q. Zheng, J.-L. Lin, J. Sun, and H.-L. Zhang, *Z. Kristallogr. NCS* **215,** 533 (2000); (d) Y.-Q. Zheng, A.-Y. Pan, and J.-L. Lin, *Z. Kristallogr. NCS* **216,** 267 (2001).
13. A. Michaelides, V. Kiritsis, S. Skoulika, and A. Aubry, *Angew. Chem. Int. Ed. Engl.* **32,** 1495 (1993).
14. (a) C. Livage, C. Egger, M. Nogues, and G. Férey, *J. Mater. Chem.* **8,** 2743 (1998); (b) C. Livage, C. Egger, and G. Férey, *Chem. Mater.* **11,** 1546 (1999); (c) Y.-Q. Zheng and J.-L. Lin, *Z. Kristallogr. NCS* **216,** 139 (2001).
15. F. E. Mabbs and D. J. Machin, "Magnetism and Transtion Metal Complexes." William Clowes & Sons Limited, London, 1973.
16. G. M. Sheldrick, "SHELXS-97, Programm zur Lösung von Kristallstrukturen," Göttingen, 1997.
17. G. M. Sheldrick, "SHELXL-97, Programm zur Verfeinerung von Kristallstrukturen," Göttingen, 1997.
18. E. A. Boudreaux and L. N. Mulay, "Theory and Applications of Molecular Paramagnetism." John Wiley & Sons, New York, 1976.